Faculty Publications, Chemistry   Chemistry

1-1-2011

Speciation, Luminescence, and Alkaline Fluorescence Quenching of 4-(2-methylbutyl)aminodipicolinic acid (H2MEBADPA)

Gilles Muller
San Jose State University, gilles.muller@sjsu.edu

A. J. Ingram
San Jose State University

A. G. Dunpal
San Jose State University

R. DiPietro
IBM-Almaden Research Center

Follow this and additional works at: https://scholarworks.sjsu.edu/chem_pub

Part of the Chemistry Commons

Recommended Citation

Speciation, Luminescence, and Alkaline Fluorescence Quenching of 4-(2-Methylbutyl)aminodipicolinic Acid (H$_2$MEBADPA)

Andrew J. Ingram,[†] Alexander G. Dunlap,[†] Richard DiPietro,[‡] and Gilles Muller*,[†]

[†]Department of Chemistry, San José State University, 1 Washington Square, San José, California 95192-0101, United States
[‡]IBM-Almaden Research Center, 650 Harry Road, San José, California 95120-6099, United States

Ⓢ *Supporting Information*

ABSTRACT: 4-(2-Methylbutyl)aminodipicolinic acid (H$_2$ME-BADPA) has been synthesized and fully characterized in terms of aqueous phase protonation constants (pK_a's) and photophysical measurements. The pK_a's were determined by spectrophotometric titrations, utilizing a fully sealed titration system. Photophysical measurements consisted of room temperature fluorescence and frozen solution phosphorescence as well as quantum yield determinations at various pH, which showed that only fully deprotonated MEBADPA^{2-} is appreciably emissive. The fluorescence of MEBADPA^{2-} has been determined to be quenched by hydroxide and methoxide anions, most likely through base-catalyzed excited-state tautomerism or proton transfer. This quenching phenomenon has been quantitatively explored through steady-state and time-resolved fluorescence measurements. Utilizing the determined pK_as and quenching constants, the fluorescent intensity of MEBADPA^{2-} has been successfully modeled as a function of pH.
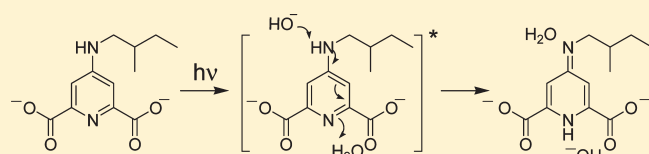
■ INTRODUCTION

Luminescent tris-dipicolinate lanthanide(III) complexes, or derivatives thereof, have been proposed as potential probes of chirality (numerous and extensive reviews are devoted to the various properties, uses, and benefits of luminescent lanthanide-(III) complexes as biomolecular probes)[1−19] due to promising features such as long lifetimes and characteristic emission, and exhibition of circularly polarized luminescence (CPL) that is dependent upon association with a chiral molecule (Figure 1).[1,20−43] In these systems an equilibrium is established between the enantiomeric Δ and Λ forms of a probing complex which can be perturbed by the addition of an optically active molecule, a phenomenon referred to as the "Pfeiffer effect".[44−47] The magnitude of this perturbation can be measured directly with CPL spectroscopy, which examines the chiroptical properties of these lanthanide(III) complexes. A high degree of polarization in the emitted light generally indicates a strong association between one enantiomer of the complex and the chiral molecule of interest, a desirable outcome when these probes are designed.[1,20,22]

Lanthanide(III) complexes of dipicolinic acid derivatives, shown in Figure 1, are promising model systems for "Pfeiffer" studies as the group in the 4-position of the ring is easily varied and allows for tuning of photophysical properties.[48,49] Also, it has been shown that probe activity can be increased and possibly made selective by altering this group.[40]

A derivative of dipicolinic acid, 4-aminodipicolinic acid, had previously been shown to form highly luminescent complexes with lanthanides,[48] and to study the efficacy of chirality probes with functionalized dipicolinates, racemic N-(2-methylbutyl)-4-
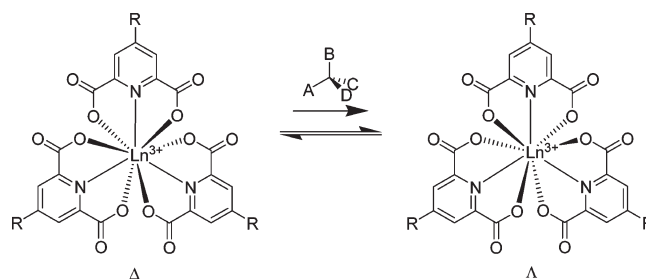
Figure 1. Proposed molecular chirality probe. Tris-dipicolinate derivatives as luminescent lanthanide(III) probes designed to detect/characterize chirality in solution. R = H, O$^-$, halogens, NH$_2$, NH(alkyl), and others.
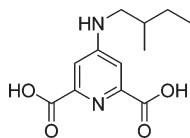
aminodipicolinic acid (hereon referred to as H$_2$MEBADPA, Chart 1) was synthesized through nucleophilic aromatic substitution of 4-chlorodipicolinic acid with racemic 2-methylbutylamine. The aqueous phase speciation and photophysical properties of this novel potential ligand, however, needed full characterization prior to complexation with lanthanides.

This characterization entailed determining the acid−base chemistry in aqueous solution, as well as studying the fluorescence and phosphorescence as a function of pH. At the outset of this study it was believed that this characterization would consist of a rather routine set of measurements, but over time it was

Chart 1. H$_2$MEBADPA

Scheme 1. Acid Dissociation Reactions

$$H_3MEBADPA^+ \rightleftharpoons H_2MEBADPA + H^+ \qquad K_{a1}$$

$$H_2MEBADPA \rightleftharpoons HMEBADPA^- + H^+ \qquad K_{a2}$$

$$HMEBADPA^- \rightleftharpoons MEBADPA^{2-} + H^+ \qquad K_{a3}$$

found that both the solution structure and photophysical properties of MEBADPA^{2-} were unique and merited separate reporting from data on the various lanthanide(III) complexes.

The acid/base chemistry of H$_2$MEBADPA was studied by spectrophotometric methods to determine each of the acid dissociation constants (pK_a's), with the data being refined by the HYPERQUAD2006 program.[50]

In terms of fluorescence, there is some history of excited processes involving aminopyridines and hydroxide, and base-catalyzed fluorescent quenching has been observed in 2- and 3-aminopyridines.[51−53] To the best of our knowledge, however, no quenching of a 4-aminopyridine by base has been reported prior to this publication. The quenching of 2- and 3-aminopyridines is believed to occur via a hydroxide catalyzed proton transfer in the excited state,[52,53] and studies of N,N-dialkyl-4-aminopyridines exhibit an excited-state charge-transfer process that moves electron density from the amino group into the pyridine ring.[54−57] This study illustrates the effect of this excited-state charge-transfer process on the reactivity of a secondary 4-aminopyridine with electron withdrawing groups adjacent to the ring.

In terms of MEBADPA's viability as part of a luminescent lanthanide probe, the most important data are the phosphorescence studies that indicate how the molecule might sensitize lanthanide luminescence and how this luminescence will depend on pH.[58−60] In these studies the phosphorescence of H$_2$MEBADPA was measured in solution frozen at 77 K at various pH to approximate the energy of the triplet state, T$_1$, for each form of the molecule. This determination was of particular interest as the energy of T$_1$ is key in the sensitization of lanthanide luminescence.[58−60]

■ EXPERIMENTAL SECTION

Chemicals used in the synthesis of H$_2$MEBADPA were purchased from Sigma-Aldrich and used without further purification with the exception of 4-chlorodipicolinic acid which was prepared according to literature methods.[61] See the Supporting Information for more specifics regarding the synthesis.

For the UV−vis and luminescence titrations, deionized water was degassed by boiling under reduced pressure and storing it under nitrogen. Stock solutions ($\approx$1 mM) of H$_2$MEBADPA were prepared by dissolution in a known volume of standardized 0.1 M NaOH or KOH and diluting to a specified volume. HCl, KOH, and NaOH standards were either purchased from Acros Organics or prepared using literature methods,[62] with the only deviation being that the HCl solutions were standardized using the prepared hydroxide solutions with bromothymol blue as an indicator. Quinine sulfate dihydrate was used as purchased from Acros Organics.

UV/vis absorbances were measured on a Varian Cary 50 Bio UV−visible spectrophotometer with an attached Cary Single Cell Peltier Accessory for temperature control. Fluorescence at
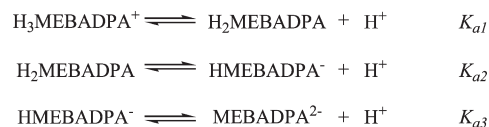
298 K and above was measured on a Varian Cary Eclipse fluorescence spectrophotometer with an attached Quantum Northwest temperature control. Phosphorescence scans (77 K) were taken on a Perkin-Elmer LS50B instrument. A Masterflex L/S compact, variable speed pump was used with Chem-Durance Bio and Tygon Chemical 2001 tubing to transfer solutions to a 1.0 cm flow cuvette (Starna Cells, Inc.) in the pK_a and quantum yield determinations. pH measurements were made with an Orion model 710A meter using an AgCl/saturated KCl electrode from Accumet calibrated using pH = 4.00 and 10.01 standards purchased from Fisher Scientific.

Fluorescent lifetimes were determined with a Horiba-Jobin-Yvon-IBH-FluoroLog-3 spectrofluorometer, adapted for time-correlated single-photon-counting (TCSPC) and multichannel scaling (MCS) measurements. A light emitting diode (LED) (Jobin-Yvon) with an output wavelength maximum at 278 nm and a pulse duration of 1.1 ns was used as the excitation source. Emission was monitored perpendicular to the excitation pulse, the spectral selection achieved by passage through the double-grating emission monochromator (2.1 nm/mm dispersion, 1200 grooves/mm). A thermoelectrically cooled single-photon-detection module (Horiba Jobin Yvon IBH, TBX-04-D) incorporating a fast-rise-time photomultiplier tube (PMT), a wide bandwidth preamplifier, and a picosecond constant-fraction discriminator was used as the detector. Signals were acquired with an IBH-DataStation-Hub photon-counting module in TCSPC mode, and data analysis was performed with the commercially available DAS-6 decay-analysis software package from Horiba Jobin Yvon IBH. Goodness of fit was assessed by minimizing the reduced χ^2 function and a visual inspection of the weighted residuals. The instrument response function was measured using a quartz 1 × 1 cm cell (Starna Cells, Inc.), where 2 drops of half-and-half (coffee creamer) was added to Millipore water to make a scattering solution. Data were collected using an IBH pulsed LED with an excitation maximum of 278 nm and a pulse duration of ~1.1 ns in TCSPC mode. The full width at half-maximum of this peak was determined to be 1.1 ns, corresponding to the LED pulse.

■ RESULTS AND DISCUSSION

Synthesis of H$_2$MEBADPA. The synthesis of H$_2$MEBADPA was achieved through nucleophilic aromatic substitution of 4-chlorodipicolinic acid with racemic 2-methylbutylamine by heating to 200 °C for 6 h in a high-pressure steel reactor. The crude was purified through an overnight esterification in methanol, utilizing thionyl chloride to create the more reactive acyl chlorides in situ. After extraction into ethyl acetate and removal of the solvent, further purification was achieved by silica gel column chromatography in hexanes:ethyl acetate, utilizing a gradient. The combined fractions containing product were deesterified by refluxing in NaOH, and H$_2$MEBADPA was then precipitated upon the addition of HCl. The compound's identity
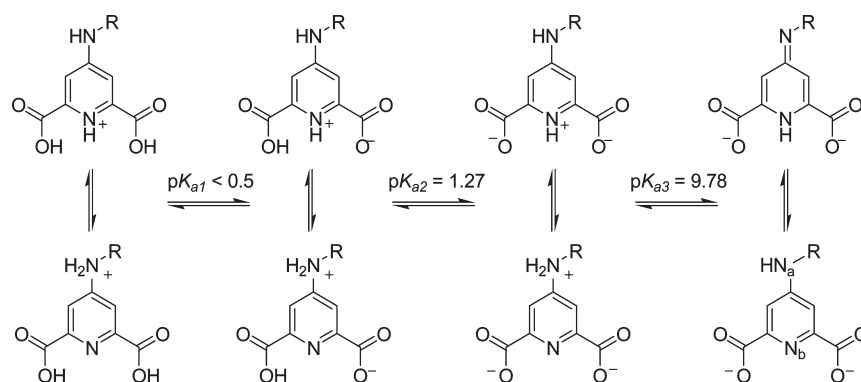
Figure 2. Proposed speciation and tautomerism of $H_2MEBADPA$. Shown are the proposed sites of protonation as well as potential tautomerism in solution. To facilitate discussion, see the bottom tautomer of fully deprotonated $MEBADPA^{2-}$ (bottom-right) for subscript designations for each nitrogen. Note that the N_a-amino tautomer (bottom-right) is expected to be predominant over the N_a-imino form above it and that the protonation corresponding to pK_{a3} is believed to occur at N_b (upper three tautomers on the left).

Table 1. pK_a Values for 4-R-Dipicolinic Acids in the Literature

Entry[ref]	-R			pK_{a1}	pK_{a2}	pK_{a3}	pK_{a4}
1[66-68]	-H		value	0.5 or below	≈ 2	≈ 4.5	-
			location	-COOH	-COOH	Pyridine	-
2[69]	(alkyne-phenyl-NH₂)		value	1.01	2.58	3.54	8.77
			location	-COOH	-COOH	Pyridine	Amine
3[70]	-OH		value	< 2	3.2-3.47	10.8-11.4	-
			location	-COOH	N or –COOH[c]	Hydroxyl	-
4[64,71]	-NH₂		value	-	1.8-2.29	9.05-9.19	-
			location	-	-COOH	Nitrogen[d]	-
5[a]	(N–H alkyl)		value	< 0.5[b]	1.27	9.78	-
			location	-COOH	-COOH	Nitrogen[d]	-

[a] This work. [b] Not actually determined but assumed to be lower than the corresponding value for DPA (entry 1). [c] There is ambiguity in the literature as to the exact site of protonation. [d] Corresponds to the protonation of the conjugated nitrogen system.

was verified by $^1H/^{13}C$ NMR, and analytically pure H_2MEBAD-PA, as assessed by HPLC, was prepared through recrystallization in hexanes/ethyl acetate (see Supporting Information for details and spectra).

Spectrophotometric Titration Results. Spectrophotometric titrations on ≈10^{-5} M solutions of $H_2MEBADPA$ were performed to quantitatively determine the pK_a's. The data were analyzed in HYPERQUAD2006 using the model shown in Scheme 1. The refinement algorithms for the program have been published previously.[50] For refining data for pK_{a2}, absorbances from 226 to 348 nm were used, and 225−325 nm absorbances were used for pK_{a3}. The results for pK_{a2} are the average of two titrations, and those for pK_{a3} are an average of three separate titrations. A value of 13.77 was used for the pK_w when NaCl was the inert electrolyte, and a value of 13.78 was used for KCl.[63]

While there appear to be four protonatable lone pairs on $MEBADPA^{2-}$, two nitrogen atoms and two carboxylates, buffering capacity and factor analysis of the UV/vis data indicated that only two protonations were observable in a pH range readily accessible to water (pH ≈ 0−15, Figure 2)

After a review of the pertinent literature[64−71] (Table 1) it was determined that this is the result of two separate phenomena: (1) the nitrogen lone pairs are connected via a conjugated π-system (Figure 3), rendering them much more basic and protonatable only once as a pair, and (2) an overall depression of the carboxylate pK_a values from the distributed positive charge, relative to dipicolinic acid (DPA, Table 1, entry 1), causes the protonation of the second carboxylate to occur at a pH lower than what is readily observable in aqueous solution. Note that the nitrogen atoms are only electronically connected if the first
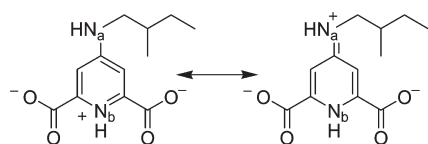
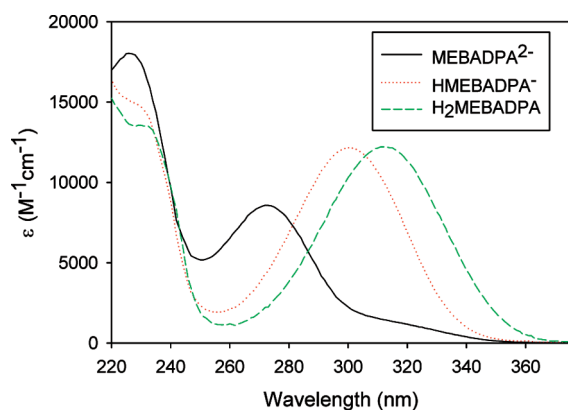**Figure 3.** Proposed Resonance Structures of HMEBADPA⁻.

Figure 4. Molar absorptivities of H₂MEBADPA. Shown here are the molar absorptivities of each form of H₂MEBDPA, as determined by spectrophotometric titration. The black curve represents MEBADPA²⁻, the dotted red line represents HMEBADPA⁻, and the dashed green line represents H₂MEBADPA.

protonation takes place at the nitrogen atom of the pyridine ring (N_b in Figure 3) rather than that of the amine (N_a).

For context, numerical results for each pK_a will first be summarized to facilitate the subsequent detailed discussion: pK_{a1} was not observed and is believed to be <0.5 corresponding to the deprotonation of the first carboxylic acid, forming the zwitterionic H₂MEBADPA; pK_{a2} has been determined as 1.27 ± 0.02 (1σ) and corresponds to the deprotonation of the final $-$COOH group forming the anion HMEBDPA⁻; finally, pK_{a3} has been determined as 9.78 ± 0.08 (1σ) and corresponds to the deprotonation of the conjugated nitrogen system, forming the dianion MEBADPA²⁻. Figure S1, Supporting Information, depicts an example of the fit of the data for a titration to determine pK_{a3}.

The molar absorptivity determined for each form of the molecule is shown in Figure 4, where the prominent bands are believed to correspond to $\pi-\pi^*$ and $n-\pi^*$ transitions. There is a large red shift as well as a moderate increase in molar absorptivity for pK_{a3}, whereas only a slight red shift results from the second protonation, indicating that this change occurs on a group peripheral to the aromatic system. Further supporting this assignment is the fact that protonation of the benzoate anion causes a similar minor red shift.[72] Worth noting is the bimodal $n-\pi^*$ peak, where a shoulder centered about 318 nm is observed. This may reflect ground-state tautomerism or a more complex electronic structure, but photophysical measurements to date have been inconclusive.

As can be seen in Figure 2, there is ambiguity in the exact structure of H₂MEBADPA in solution. While the bulk of the protonation is believed to take place at N_b,[65] there still exists the possibility of some amount of tautomerism in solution. ¹³C NMR studies have been attempted, but the solubility of HMEBADPA⁻ in D₂O is too low to obtain useful spectra.

Comparing the determined values with those of analogs in the literature (see Table 1), we can make a few observations. As expected, the *N*-alkyl group increased the basicity of the nitrogen pair relative to the value for 4-aminodipicolinic acid (entry 4 in Table 1). Also worth mentioning is that the nitrogen pair has been shown to be separately protonated and less basic in a system where the amino group is electronically isolated from the pyridine ring (Table 1, entry 2). Finally, it appears that the addition of the amino group para to the nitrogen of the pyridine ring drastically increases the acidity of the carboxylic functions relative to DPA (Table 1, entry 1), as neither in this nor previous work on 4-aminodipicolinic acid was the protonation of the second carboxylic acid observed (see entries 4 and 5 in Table 1).

Fluorescence and Alkaline Quenching of H₂MEBADPA. The quantum yield (Φ) of a luminescent species is defined as in eq 1 and represents the ratio of the number of photons emitted by a chromophore to the number of photons absorbed.

$$\Phi = \frac{(\text{photons}_{\text{em}})}{(\text{photons}_{\text{abs}})} \quad (1)$$

Because this property is exceptionally difficult to measure directly, the quantum yields of the various forms of H₂MEBAD-PA were measured using the dilute solution method[73−76] (Abs < 0.01) against a known reference, quinine sulfate in H₂SO₄ ($\Phi_R = 0.54$[74]), using eq 2 to compare the reference and sample. $\int I d\lambda$ is the numerically integrated intensity from the fluorescence spectra, I is the luminescent intensity at the excitation wavelength, A is the absorbance at the excitation wavelength, and n is the index of refraction of the solution. The subscript R denotes reference.

$$\frac{\Phi_{\text{sample}}}{\Phi_R} = \left(\frac{\int I_{\text{sample}} \, d\lambda}{\int I_R \, d\lambda}\right)\left(\frac{I_{R,\text{exc}}}{I_{\text{sample,exc}}}\right)\left(\frac{A_{R,\lambda_{\text{exc}}}}{A_{\text{sample},\lambda_{\text{exc}}}}\right)\left(\frac{n_{\text{sample}}}{n_R}\right)^2 \quad (2)$$

The determined quantum yields of H₂MEBADPA are displayed as a function of pH along with the speciation in Figure 5. As can be seen, there was no appreciable fluorescence for either the zwitterionic H₂MEBADPA or singly anionic HMEBADPA⁻. The increase of quantum yield from pH 8 to 11 clearly corresponded to the formation of the dianion MEBADPA²⁻, the only fluorescent species. The lack of emission in either H₂MEBADPA or HMEBADPA⁻ is most likely attributed to photoinduced tautomerism and/or proton transfer to solvent, both observed in other heterocyclic zwitterions,[77−79] or through deactivation pathways involving structural conformations observed in similar (diakylamino)pyridine derivatives.[54−57] Of the two potential deactivation mechanisms, the former is the most likely cause, as fluorescence is observed upon removal of the labile proton (pH > 8), indicating its intimate involvement in the quenching process. The dramatic decrease of fluorescence above pH 12 has been determined to be the result of dynamic quenching by hydroxide anions. Similar hydroxide-catalyzed quenching has also been reported for 2- and 3-aminopyridines,[52,53] indicating that this process is not unique to MEBADPA²⁻, merely not well-studied for these systems.

Fluorescence quenching by an analyte, Q, in solution is generally described by the Stern−Volmer equation (3),[80] where I is the observed intensity at a given wavelength, I_o is the intensity at that same wavelength if there were no quencher, K_{SV} is the Stern−Volmer quenching constant, and [Q] is the concentration
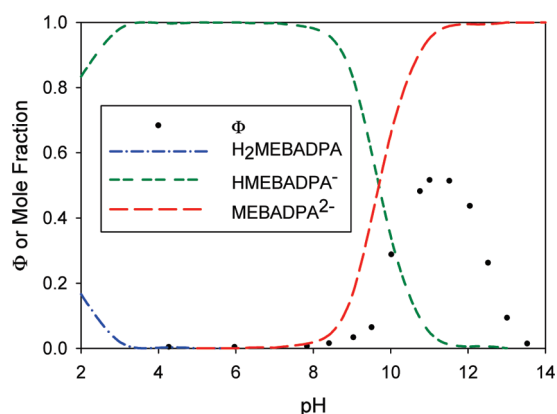
Figure 5. Φ overlaid with speciation curves. Shown here are the speciation curves for $H_2MEBADPA$ overlaid with the quantum yield determined at various pH. The dark circles are the quantum yields determined at each pH value, the blue dashed and dotted lines are the mole fraction of $H_2MEBADPA$, the dotted green line is the mole fraction of $HMEBADPA^-$, and the dashed red line represents the mole fraction of $MEBADPA^{2-}$. This clearly shows that $MEBADPA^{2-}$ is the only appreciably luminescent species, and that the quenching observed above pH $\sim$ 11.8 is caused by something besides speciation.

of the quencher. If this quenching is dynamic, where a collision event between the excited fluorophore and the quencher must occur before emission, there is an additional lifetime effect that can be expressed as in eq 4, where k_q is the bimolecular quenching rate constant, τ_o is the unquenched lifetime, and τ is the observed lifetime in the presence of quencher. Note that in dynamic quenching, k_q, and subsequently K_{SV}, depends on the number of collisions per unit time and should increase as a function of temperature.

$$\frac{I_o}{I} = 1 + K_{SV}[Q] \tag{3}$$

$$\frac{I_o}{I} = 1 + k_q\tau_o[Q] = \frac{\tau_o}{\tau} \tag{4}$$

Equation 3 makes no distinction between static and dynamic quenching, whereas eq 4 only applies to dynamic. Static quenching generally involves an equilibrium reaction with the ground-state chromophore that forms a nonluminescent species. In this way H_3O^+ can be thought of as a static quencher of $MEBADPA^{2-}$, as $HMEBADPA^-$ is not a fluorescent species.

In collisional quenching, however, there is no reaction with the ground-state chromophore. Upon excitation, however, the quenching agent can react with any molecule in the excited state prior to fluorescence. If a successful collision event occurs before emission, lower (or modified) intensity is observed. The need for a successful collision event before fluorescence causes the magnitude of quenching to be dependent on τ_o, as a chromophore with a longer lifetime leaves more time for collision events to occur. Thus, to gain insight regarding the mechanism, it was important to ascertain if the quenching affected the measured lifetime.

To ensure this quenching was the result of OH^-, control experiments in concentrated (>1 M) solutions of NaCl, NaOH, HCO_3^-/CO_3^-, and Na_2SO_4 demonstrated that $MEBADPA^{2-}$, in these conditions, was selectively quenched by hydroxide. Subsequent luminescence studies at different concentrations of

hydroxide found that the decrease in luminescence is very well described by the modified Stern−Volmer equation (5) with $K_{SV} = 43.4 \pm 2.1$ M^{-1} (Figure 6). Note that eq 5 is slightly modified from the canonical Stern−Volmer eq 3 to account for the fact that an appreciable amount of OH^- was necessary to ensure complete formation of $MEBADPA^{2-}$. This made it so I_o could not be measured directly and was treated as a fitting parameter. The fluorescence data from all wavelengths from 365 to 475 nm were fit to eq 5, and the K_{SV} for a run is averaged from the fits of each of these wavelengths. The reported value is an average of two separate runs.

$$\frac{1}{I} = \frac{K_{SV}}{I_o}[Q] + \frac{1}{I_o} \tag{5}$$

As I_o was determined from this fit, it was possible to obtain spectra for the unquenched fluorescence of $MEBADPA^{2-}$ from the measurements used to determine the Φ as a function of pH. The average of the numerical integration of these spectra was then used to approximate the value for the quantum yield of unquenched $MEBADPA^{2-}$, yielding $\Phi_o = 0.72$ (observed $\Phi_{max.} = 0.51$ in Figure 5). While, due to the alkaline pH necessary to form $MEBADPA^{2-}$, it is impossible to achieve a quantum yield this high in aqueous solution, this represents the theoretical quantum yield in absence of the quenching effect.

Two experiments were performed to determine if the alkaline quenching of $MEBADPA^{2-}$ was static or dynamic. The first experiment determined the temperature dependence of the luminescence, and the second was a series of lifetime measurements aimed at determining the bimolecular quenching constant, k_q.

The temperature study found that the luminescence decreased linearly as the temperature increased, as expected from a dynamic process (Figure S2, Supporting Information).[80] If the quenching was instead due to an additional deprotonation of $MEBADPA^{2-}$ (Scheme 2), the temperature effect would have been described by an equation similar to (6), derived from simple expressions for Beer's Law, free energy, equilibrium, mass action, and mass conservation; where I_λ is the fluorescent intensity at wavelength λ, ε_λ is the emissivity of $MEBADPA^{2-}$ at wavelength λ, $[MEBADPA^{2-}]_{tot}$ is the total concentration of all species of $H_2MEBADPA$, ΔG is the free energy of the association reaction, and R is the gas constant. Note that eq 6 does not account for the temperature dependence of K_w.

$$I_\lambda = \varepsilon_\lambda[MEBADPA^{2-}] = \frac{[MEBADPA^{2-}]_{tot}}{[H^+] + e^{\Delta G/-RT}} \tag{6}$$

The near 33% decrease in intensity observed at 60 °C relative to 25 °C is not easily rationalized by eq 6, and therefore it is not a suitable model for this quenching process. These data strongly indicated that the quenching was not static but, in fact, dynamic.

In the lifetime measurements, each measurement above pH 12 was found to be well fit by a single exponential and the resulting lifetime decreased as pH increased, again well described by a modified Stern−Volmer equation (7) (Figure 7). This also confirmed a dynamic quenching model, as a static process would have shown no correlation between lifetime and concentration of quencher. The bimolecular quenching rate constant determined from eq 7 was found to be 4.24×10^9 M^{-1}s^{-1}, which is of the correct magnitude to describe a collisional mechanism ($\approx 10^{10}$).[80−84] Equation 7 also allowed for an approximation of the unquenched lifetime of $MEBADPA^{2-}$, where $\tau_o \approx 5.6$ ns.

7916

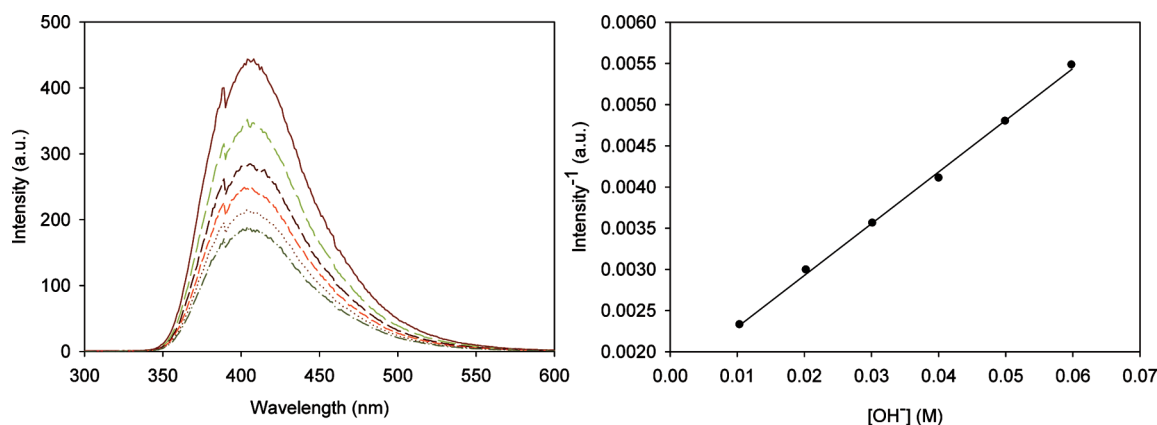dx.doi.org/10.1021/jp201209k |*J. Phys. Chem. A* 2011, 115, 7912−7920

Figure 6. Hydroxide quenched fluorescence of MEBADPA^{2-} and modified Stern–Volmer plot. The left graph shows the decrease in the fluorescence of MEBADPA^{2-} upon addition of hydroxide. The right graph plots the inverse of the intensity at 400 nm as a function of [OH$^-$] and shows the plotted linear relationship ($R^2 = 0.998$). [MEBADPA^{2-}] is a constant 5×10^{-5} M, the pH is varied from ~12 to 13, and μ is kept at a constant 0.10 M with NaCl.

Scheme 2. Unlikely Deprotonation Reaction

Figure 8. Proposed phototautomerism. Shown here is a proposed mechanism for OH$^-$ specific quenching, where the hydroxide catalyzes an excited-state proton transfer from N$_a$ to N$_b$. The product is expected to nonradiatively decay through vibrational coupling or further reaction with solvent.
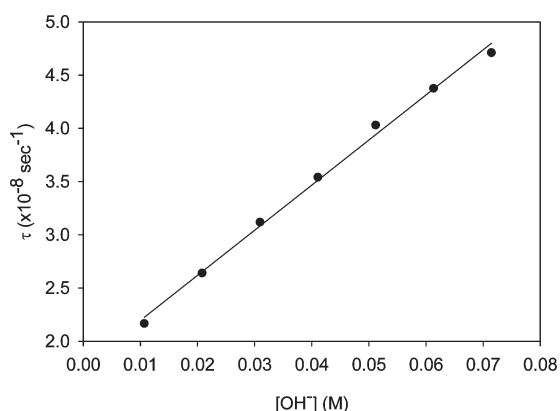

Figure 7. Modified lifetime Stern–Volmer plot. The inverse of measured MEBADPA^{2-} lifetimes is plotted against [OH$^-$]. It shows near-linear behavior ($R^2 = 0.996$) that indicates collisional quenching.

$$\frac{1}{\tau} = \frac{1}{\tau_o} + k_q[\text{OH}^-] \quad (7)$$

While a detailed determination and discussion of the quenching mechanism is out of the scope of this particular study, there are two likely possibilities. The most probable is a base-catalyzed excited-state tautomerism or proton-transfer mechanism[51,52,71] (Figure 8), although the more common charge-transfer mechanism associated with anionic quenching was considered (Figure S4, Supporting Information).[81–84]

The latter seems promising, but in light of the control experiments that showed that the common electron-transfer quenchers, NaCl and Na$_2$SO$_4$,[81–84] did not observably alter the fluorescence, it is difficult to assume this type of mechanism. NaSCN and Na$_2$SO$_3$ were also tested, but each had an appreciable absorption at the excitation wavelength, 273 nm, which affected the fluorescence through the inner filter effect.[85]
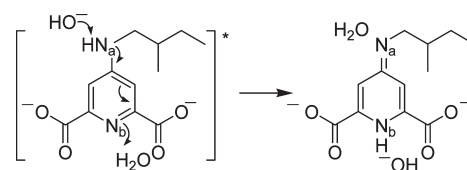
The tautomerism mechanism consists of a base catalyzed transfer of a proton from N$_a$ to N$_b$ (Figure 8). This transfer can be rationalized if the electron density in the excited state lies mostly on N$_b$, as observed in N,N-diakyl-4-aminopyridines,[54–57] making N$_b$ more basic upon excitation. While this process is extremely similar to H$_2$O-mediated intramolecular proton transfer observed in other heterocycles,[77–79] it appears that water is not a strong enough nucleophile to promote the reaction, giving the observed selectivity for hydroxide. Such a mechanism in MEBADPA^{2-} would indirectly support a proton-transfer mechanism as the reason for the lack of fluorescence in HMEBADPA$^-$ and H$_2$MEBADPA.

To confirm the nucleophilic aspect of the quenching mechanism, the dimethyl ester of H$_2$MEBADPA, Me$_2$MEBADPA, was prepared by dissolving the solid diacid in anhydrous MeOH. The compound was allowed to esterify over a matter of days before determining the effect of NaOMe on the fluorescence. As shown in Figure S3, Supporting Information, the decrease in fluorescence could not be described solely by dissolution from the added volume of NaOMe solution. If the dimethyl diester is taken to be positive and singly protonated in neutral MeOH (i.e., it exists as HMe$_2$MEBADPA$^+$), then the initial increase of fluorescence would correspond to the formation of an emissive, neutral Me$_2$MEBADPA. The subsequent decrease in fluorescence is again well described by another modified Stern–Volmer equation that accounts for dissolution (8), where I is the emission at a given wavelength and addition of NaOMe, ε_λ is the emissivity of Me$_2$MEBADPA at the designated wavelength, [Me$_2$MEBADPA] is the concentration of Me$_2$MEBADPA at a given point, K_{SV} is the Stern–Volmer quenching constant of

Table 2. Photophysical Properties of MEBADPA^{2-}

	value $\pm 1\sigma$
$K_{SV,NaOH}{}^a$	43.4 ± 2.1 M^{-1}
$K_{SV,NaOH}{}^b$	23.9 ± 1.0 M^{-1}
$K_{SV,NaOMe}{}^a$	7.18 ± 0.10 M^{-1}
$k_{q,NaOH}{}^b$	$(4.24 \pm 0.12) \times 10^9$ M^{-1} s^{-1}
$\tau_o{}^b$	5.64 ± 0.18 ns
$\Phi_o{}^a$	0.72
pH$_{max. fluor}{}^a$	11.07

^{a} Determined using steady-state methods. ^{b} Determined using time-resolved methods.

NaOMe for Me$_2$MEBADPA in MeOH, and [NaOMe] is the concentration of NaOMe at a given point. Fitting the data beyond 1 mL of added 0.5 M NaOMe yields $K_{SV} = 7.10 \pm 0.10$ M^{-1} (1σ). The difference in values from water to methanol could be attributed to a decreased τ_o in MeOH and/or the more sterically hindered $^-$OMe nucleophile.

$$I = \varepsilon_\lambda \frac{[\text{Me}_2\text{MEBADPA}]}{1 + K_{SV}[\text{NaOMe}]} \qquad (8)$$

A final piece of evidence in support of the tautomerism mechanism is the well studied charge-transfer process observed in N,N-dialkyl-4-aminopyridines.[54−57] In this process, electron density is transferred from the amino group to the pyridine nitrogen as the molecule enters the excited state. It is conceivable that the introduction of electron withdrawing carboxylic groups ortho to N$_b$ would enhance the charge-transfer process and moving from a tertiary to a secondary amine would allow for proton transfer.

Another possibility would be that deprotonation of N$_a$ could occur without tautomerism, rather than the proton transfer described above. This is considered to be unlikely as it involves the formation of a rather unstable imine/amide resonance pair as a product, rather than the imine/amine tautomer.

A Strickler−Berg type analysis[86,87] was also attempted to determine τ_o indirectly from the absorption and emission spectra; however, this approach vastly underestimated the value of τ_o to be 0.1 ns as well as completely insensitive to [OH$^-$] (see the Supporting Information for more details). As the derivation of the Strickler−Berg equation is dependent on the assumption that the structure of the excited state is identical to that of the ground state,[86,87] this analysis further supports the charge-transfer mechanism as the amine bound groups are expected to rotate to be near orthogonal to the plane of the pyridine in the excited state.[54−57]

It should be noted that the time-resolved measurements and steady-state measurements of K_{SV} do not quantitatively agree (Table 2). It is unclear whether this might be attributed to experimental details or if there is a mechanistic explanation for this phenomenon. In either case, the values found using steady-state methods are very consistent and repeatable, as shown below.

To test whether the fluorescence could be successfully described by the determined equilibrium and quenching constants, the intensity was mathematically modeled as a function of pH and then empirically measured. If it is assumed that intensity is linear with concentration, and the [H$_2$MEBADPA] is negligible at any pH where there is an appreciable [MEBADPA^{2-}], as
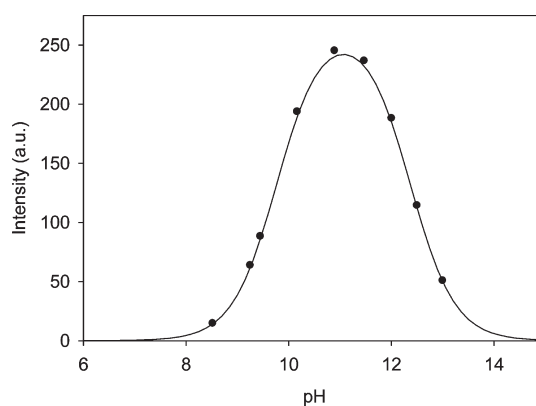

Figure 9. Intensity vs pH. Shown here is both the theoretical and measured fluorescence intensity (at 400 nm) of 3.2×10^{-5} M solutions of H$_2$MEBADPA at various pH. The dark circles are measured intensities, and the curve calculated from eq 9 treating K_{SV} (as determined by steady-state methods) and pK_{a3} as constants and adjusting bk_λ to find the optimum fit of the data ($R^2 = 0.978$).

indicated by the determined pK_a values, then the expression (9) for fluorescent intensity as a function of pH is obtained. This expression incorporates the Stern−Volmer quenching model as well as the protonation of MEBADPA^{2-} to the nonemissive HMEBADPA$^-$, where b is a constant representing instrument parameters, k_λ is the emissivity of MEBADPA^{2-} at the wavelength λ, K_{a3} is the acid dissociation constant as defined in Scheme 1, and [MEBADPA$_{tot}$] is the total concentration of all species of H$_2$MEBADPA.

$$I = bk_\lambda \frac{K_{a3}[\text{MEBADPA}_{tot}]}{(10^{-pH} + K_{a3})\left(1 + K_{SV}\dfrac{K_w}{10^{-pH}}\right)} \qquad (9)$$

As can be seen in Figure 9, when fitted to experimental data, eq 9 very accurately describes the fluorescence of H$_2$MEBADPA as a function of pH. Note that only bk_λ was adjusted while fitting the experimental data, and all other values either were calculated from solution specifications or were constants determined in the steady-state measurements (see Table 2). Setting the derivative of eq 9 equal to zero allows for an analytical solution of the pH where maximum emission is observed (pH$_{max.}$ = 11.07).

Determination of the Energy of the Triplet State. In luminescent lanthanide(III) complexes, the most common method for efficient energy transfer between a ligand and a lanthanide(III) ion highly depends on the difference of energy between the triplet state of a ligand, T$_1$, and the accepting metal energy level.[58−60] For the purposes of this discussion, Eu(III) and Tb(III) will be focused on, as they tend to have the larger quantum yields and longer luminescent lifetimes desired for probes.[88] In this sensitization process, energy from an electron in the T$_1$ state is transferred to promote the lanthanide into an excited atomic state (the term states of accepting metal energy levels vary between lanthanides, but Eu(III) and Tb(III) tend to accept in the ^{5}D$_j$, where the accepting j level depends on the energy of T$_1$[89]), from which they can radiatively decay into the lower atomic states. Each f-block element has a separate set of energy levels, as well as particular accepting states, that are generally independent of their chemical environment, giving each lanthanide(III) ion's characteristic luminescence. The

optimum difference in energy between the metalated ligand's donor T_1 level and lanthanide(III)'s acceptor level is generally 2000—3500 cm^{-1} to ensure metal-based luminescence and avoid back-transfer.[59,89] While the energy of T_1 will change upon metalation, the value for the free ligand is important to gain insight on the intersystem crossing transfer as a baseline value for later comparison and to confirm that lanthanide luminescence is plausible (i.e., the energy of T_1 is sufficiently greater than the energy of the accepting metal energy level).

To determine the energy of the triplet state, phosphorescence measurements at 77 K were performed on solutions of H_2ME-BADPA at varying pH. The strong phosphorescence of MEBADPA^{2-} at pH $\approx$ 12.5 was recorded as a broad peak centered at 450 nm (Figure S4, Supporting Information), whereas spectra for H_2MEBADPA and HMEBADPA$^-$ were unable to be measured as the signal was so low it could not be isolated from artifacts in the instrumentation and/or cuvette. Apparently, the processes responsible for quenching the emission of H_2/HMEBADPA$^{/-}$ at 298 K are not sufficiently slowed at 77 K to allow for readily measurable phosphorescence.

Using a set of 11 Gaussian curves to *pseudo*-approximate the vibrational structure of the phosphorescence, the energy of T_1 was estimated as 27 000 cm^{-1} above S_0, the ground state. This corresponds well with the accepting levels for most lanthanides, which tend to be in the range 20 000—25 000 cm^{-1} for metal-based emission,[58] and bodes particularly well for any complexes of Tb(III) that tend to prefer an energy of 23 000 cm^{-1} or greater.[89] If the maximum of the phosphorescence peak (449 nm) is taken as the energy of T_1, a value of 22 000 cm^{-1} is obtained. This is also suitable for sensitization of some lanthanides. As the energy of T_1 is only expected to change by $\approx\pm1000$ cm^{-1} upon metalation, based on similar ligands and lanthanide(III) complexes,[60] these measurements indicate that MEBADPA^{2-} should sensitize the luminescence of lanthanide-(III) cations and are therefore worth pursuing as ligands for potential molecular probes.

CONCLUSIONS

The novel dipicolinic acid derivative H_2MEBADPA has been synthesized and fully characterized in terms of speciation and photophysical properties. Curiously, only two pK_a's are observable in aqueous solution, which has been attributed to a single conjugated diamine system as well as a very acidic carboxylic acid group.

Of the various forms of the molecule, only the fully deprotonated MEBADPA^{2-} exhibits fluorescence. It has been determined that its fluorescence is quenched in alkaline solution most likely by a base-catalyzed proton-transfer mechanism. The triplet state of the fully deprotonated species has also been determined in frozen solution.

The speciation and photophysical constants have been used to successfully and quantitatively model the fluorescence of MEBADPA^{2-} as a function of pH. This knowledge can be used to predict and explain how complexes of this molecule with different lanthanides might behave in terms of overall luminescence as well as how this luminescence might depend on pH and ligand:metal ratios. These data will be of utmost importance when potential molecular probes are constructed with this and similar 4-amino analogs of dipicolinic acid. Of key interest are the structural and photophysical properties of the complexes of chiral, rather than racemic, H_2MEBADPA.

ASSOCIATED CONTENT

S **Supporting Information.** Additional figures including titration examples, the temperature dependence of the quenching, the quenching by NaOMe, and the absorbance, NMR, fluorescence, and phosphorescence of MEBADPA^{2-}, along with detailed experimental procedures, mathematical derivations, and the Strickler—Berg analysis are available. This material is available free of charge via the Internet at http://pubs.acs.org.

AUTHOR INFORMATION

Corresponding Author
*E-mail: gilles.muller@sjsu.edu.

ACKNOWLEDGMENT

REFERENCES

(1) Muller, G. *Dalton Trans* **2009**, 9692–9707.
(2) Shinoda, S.; Tsukube, H. *Analyst* **2011**, *136*, 431–435.
(3) Piguet, C.; Bünzli, J.-C. G. In *Handbook on the Physics and Chemistry of Rare Earths*; Gschneidner, K., Jr., Bünzli, J. G., Pecharsky, V. G., Eds.; North-Holland Publishing Co.: Amsterdam, 2010; Vol. 30, p 301.
(4) Bünzli, J.-C. G. *Chem. Rev.* **2010**, *110*, 2729–2755.
(5) New, E. J.; Parker, D.; Smith, D. G.; Walton, J. W. *Curr. Opin. Chem. Biol.* **2010**, *14*, 238–246.
(6) Bünzli, J.-C. G. *Chem. Lett.* **2009**, *38*, 104–109.
(7) Moore, E. G.; Samuel, A. P. S.; Raymond, K. N. *Acc. Chem. Res.* **2009**, *42*, 542–552.
(8) Thibon, A.; Pierre, V. C. *Anal. Bioanal. Chem.* **2009**, *394*, 107–120.
(9) dos Santos, C. M. G.; Harte, A. J.; Quinn, S. J.; Gunnlaugsson, T. *Coord. Chem. Rev.* **2008**, *252*, 2512–2527.
(10) Sturza, C. M.; Boscencu, R.; Nacea, V. *Farmacia* **2008**, *LVI*, 326–338.
(11) de Bettencourt-Dias, A. *Curr. Org. Chem.* **2007**, *11*, 1460–1480.
(12) Bünzli, J.-C. G.; Comby, S.; Chauvin, A.; Vandevyver, C. D. B. *J. Rare Earths* **2007**, *25*, 257–274.
(13) Bünzli, J.-C. G. *Acc. Chem. Res.* **2006**, 53–61.
(14) Parker, D.; Bretonnière, Y. In *Molecular Imaging*; Bogdanov, A. A. J., Licha, K., Eds.; Springer: Berlin, Heidelberg, 2005; Vol. 49, pp 123—146.

(15) Parker, D. *Chem. Soc. Rev.* **2004**, *33*, 156–165.

(16) Parker, D.; Williams, J. A. G. The Lanthanides and their Interactions with Biosystems. In *Metal Ions in Biological Systems*; Sigel, A., Sigel, H., Eds.; Marcel Dekker Inc: New York, 2003; Vol. 40, pp 233−280.

(17) Montgomery, C. P.; Murray, B. S.; New, E. J.; Pal, R.; Parker, D. *Acc. Chem. Res.* **2009**, *42*, 925–937.

(18) New, E. J.; Parker, D; Peacock, R. D. *Dalton Trans.* **2009**, 672–679.

(19) Bünzli, J.-C. G.; Chauvin, A.; Vandevyver, C. D. B.; Bo, S.; Comby, S. *Ann. N. Y. Acad. Sci.* **2008**, *1130*, 97–105.

(20) Riehl, J. P.; Muller, G. Circularly Polarized Luminescence Spectroscopy and Emission-Detected Circular Dichroism. In *Advances in Chiroptical Methods*; Berova, N., Polavarapu, P., Nakanishi, K., Woody, R., Eds.; John Wiley & Sons, Inc., in press.

(21) Parker, D.; Dickins, R. S.; Puschmann, H.; Crossland, C.; Howard, J. A. K. *Chem. Rev.* **2002**, *102*, 1977–2010.

(22) Riehl, J. P.; Muller, G. In *Handbook on the Physics and Chemistry of Rare Earths*; Gschneidner, K. A., Jr., Bünzli, J.-C. G., Pecharsky, V. G., Eds.; North-Holland Publishing Co.: Amsterdam, 2005; Vol. 34, p 289.

(23) Crassous, J. *Chem. Soc. Rev.* **2009**, *38*, 830–845.

(24) Muller, G.; Riehl, J. P. *J. Fluoresc.* **2005**, *15*, 553–558.

(25) Tsukube, H.; Shinoda, S. *Chem. Rev.* **2002**, *102*, 2389–2403.

(26) Berova, N.; Nakanishi, K.; Woody, R. W. *Circular Dichroism: Principles and Applications*; Wiley-VCH: New York, 2000; p 912.

(27) Huskowska, E.; Riehl, J. P. *Inorg. Chem.* **1995**, *34*, 5615–5621.

(28) Brittain, H. G. *Pract. Spectrosc.* **1991**, *12*, 179–200.

(29) Brittain, H. G. *J. Coord. Chem.* **1989**, *20*, 331–347.

(30) Hilmes, G. L.; Çoruh, N; Riehl, J. P. *Inorg. Chem.* **1988**, *27*, 1136–1139.

(31) Yan, F.; Copeland, R. A.; Brittain, H. G. *Inorg. Chem.* **1982**, *21*, 1180–1185.

(32) Brittain, H. G. *Dalton Trans.* **1984**, *7*, 1367–1370.

(33) Brittain, H. G. *Inorg. Chem.* **1981**, *20*, 3007–3013.

(34) Wu, S.; Hilmes, G. L.; Riehl, J. P. *J. Phys. Chem.* **1989**, *93*, 2307–2310.

(35) Çoruh, N.; Hilmes, G. L.; Riehl, J. P. *Inorg. Chem.* **1988**, *27*, 3647–3651.

(36) Hilmes, G. L.; Riehl, J. P. *J. Phys. Chem.* **1983**, *87*, 3300.

(37) Maradas, J. S.; Brittain, H. G. *Inorg. Chem.* **1980**, *19*, 3842–3845.

(38) Yan, F.; Brittain, H. G. *Polyhedron* **1982**, *1*, 195–199.

(39) Huskowska, E.; Riehl, J. P. *Inorg. Chem.* **1995**, *34*, 5615–5621.

(40) Moussa, A.; Pham, C.; Bommireddy, S.; Muller, G. *Chirality* **2009**, *21*, 497–506.

(41) Muller, F.; Muller, G.; Riehl, J. P. *Chirality* **2007**, *19*, 826–832.

(42) Muller, G.; Muller, F.; Maupin, C. L.; Riehl, J. P. *Chem. Commun.* **2005**, 3615–3617.

(43) Gawryszewka, P.; Legendziewicz, J.; Ciunik, Z.; Esfandiari, N.; Muller, G.; Piguet, C.; Cantuel, M.; Riehl, J. P. *Chirality* **2006**, *18*, 406–412.

(44) Kirschner, S. *J. Indian Chem. Soc.* **1974**, *LI*, 28–31.

(45) Pfeiffer, P.; Nakasuka, Y. *Chem. Ber.* **1933**, *66B*, 415–418.

(46) Pfeiffer, P.; Quehl, K. *Chem. Ber.* **1932**, *65*, 560–565.

(47) Pfeiffer, P.; Quehl, K. *Chem. Ber.* **1931**, *64*, 2667–2671.

(48) Lamture, J. B.; Zhou, Z. H.; Kumar, A. S.; Wensel, T. G. *Inorg. Chem.* **1995**, *34*, 864–869.

(49) Gassner, A.; Duhot, C.; Bünzli, J.-C. G.; Chauvin, A. *Inorg. Chem.* **2008**, *47*, 7802–7812.

(50) Gans, P.; Sabatini, A.; Vacca, A. *Talanta* **1996**, *43*, 1739–1753.

(51) Babiak, S.; Testa, A. C. *J. Phys. Chem.* **1976**, *80*, 1882–1885.

(52) Fujimoto, A.; Ando, H.; Inuzuka, K.; Nakamura, J. *Bull. Chem. Soc. Jpn.* **1993**, *66*, 414–420.

(53) Zhang, F.; Ai, Y.; Luo, Y.; Fang, W. *J. Chem. Phys.* **2009**, *130*, 144315.

(54) Szydłowska, I.; Kubicki, J.; Herbich, J. *Photochem. Photobiol.* **2005**, *4*, 106–112.

(55) Herbich, J.; Waluk, J. *Chem. Phys.* **1994**, *188*, 247–265.

(56) Szydłowska, I.; Kyrychenko, A.; Nowacki, J.; Herbich, J. *Phys. Chem. Chem. Phys.* **2003**, *5*, 1032–1038.

(57) Szydłowska, I.; Nowacki, J.; Herbich, J. *J. Photochem. Photobiol. A* **2010**, *209*, 135–146.

(58) Bünzli, J.-C. G.; Piguet, C. *Chem. Soc. Rev.* **2005**, *34*, 1048–1077.

(59) Steemers, F. J.; Verboom, W.; Reinhoudt, D. N.; van der Tal, J. E. B.; Verhoeven, J. W. *J. Am. Chem. Soc.* **1995**, *117*, 9408–9414.

(60) Muller, G.; Schmidt, B.; Jiricek, J.; Hopfgartner, G.; Riehl, J. P.; Bünzli, J.-C. G.; Piguet, C. *J. Chem. Soc., Dalton Trans.* **2001**, 2655–2662.

(61) Kurosaki, H.; Sharma, R. K.; Aoki, S.; Inoue, T.; Okamoto, Y.; Sugiura, Y.; Doi, M.; Ishida, T.; Otsuka, M.; Goto, M. *J. Chem. Soc., Dalton Trans.* **2001**, 441–447.

(62) Harris, D. C. *Quantitative Chemical Analysis*, 7th ed.; Freeman: New York, 2007.

(63) Harned, H. S.; Owen, B. B. *The Physical Chemistry of Electrolytic Solutions*, 3rd ed.; Reinhold Publishing Corp.: New York, 1958; pp 634−649, 752−754.

(64) Anderegg, G.; Bottari, E. *Helv. Chim. Acta* **1965**, *48*, 887.

(65) Cruege, F. *Bull. Soc. Chim. Fr.* **1970**, *11*, 3889.

(66) Crans, D. L.; Kiss, Y. *Inorg. Chem.* **2000**, *39*, 4409.

(67) Funahashi, S.; Haraguchi, K.; Tanaka, M. *Inorg. Chem.* **1977**, *16*, 1349.

(68) Faucherre, J.; Petitfaux, C.; Charlier, B. *Bull. Soc. Chim. Fr.* **1967**, 1091.

(69) Platas, C.; Piguet, C.; Andre, N.; Bünzli, J.-C. G. *J. Chem. Soc., Dalton Trans.* **2001**, 3084.

(70) Bag, S.; Fernando, Q.; Freiser, H. *Inorg. Chem.* **1962**, *1*, 887.

(71) Blasius, E.; Brazio, B. *Ber. Bunsen-Ges. Phys. Chem.* **1964**, *68*, 52.

(72) Pavia, D. L.; Lampman, G. M.; Kriz, G. S. *Introduction to Spectroscopy*, 3rd ed.; Saunders College Publisher (Elsevier): Amsterdam, 2001.

(73) Melhuish, W. H. *J. Phys. Chem.* **1961**, *65*, 229–235.

(74) Eastman, J. W. *Photochem. Photobiol.* **1967**, *6*, 55–12.

(75) Chauvin, A.; Gumy, F.; Imbert, D.; Bünzli, J.-C. G. *Spectrosc. Lett.* **2004**, *37*, 517–532.

(76) Aebischer, A.; Gumy, F.; Bünzli, J.-C. G. *Phys. Chem. Chem. Phys.* **2009**, *11*, 1346–1353.

(77) Bardez, E.; Devol, I.; Larrey, B.; Valeur, B. *J. Phys. Chem. B* **1997**, *101*, 7786–7793.

(78) Bahers, T. L.; Adamo, C.; Ciofini, I. *J. Phys. Chem. A* **2010**, *114*, 5932–5939.

(79) Drössler, P.; Holzera, W.; Penzkofera, A.; Hegemann, P. *Chem. Phys.* **2002**, *282*, 429–439.

(80) Lacowicz, J. R. *Principles of Fluorescence Spectroscopy*, 2nd ed.; Kluwer Academic: New York, 1999.

(81) Legg, K. D.; Hercules, D. M. *J. Phys. Chem.* **1970**, *74*, 2114–2118.

(82) Shizuka, H.; Nakamura, M.; Morlta, T. *J. Phys. Chem.* **1980**, *84*, 989–994.

(83) Fabbrizzi, L.; Licchelli, M.; Rabaioli, G.; Taglietti, A. *Coord. Chem. Rev.* **2000**, *205*, 85–108.

(84) Swinburne, A. N.; Paterson, M. J.; Beeby, A.; Steed, J. W. *Org. Biomol. Chem.* **2010**, *8*, 1010–1016.

(85) Kubista, M.; Sjöback, R.; Eriksson, S.; Albinsson, B. *Analyst* **1994**, *119*, 417–419.

(86) Strickler, S. J.; Berg, R. A. *J. Chem. Phys.* **1962**, *37*, 814–822.

(87) Birks, J. B.; Dyson, D. J. *Proc. R. Soc. London A* **1963**, *275*, 135–148.

(88) Moore, E. G.; Samuel, A. P. S.; Raymond, K. N. *Acc. Chem. Res.* **2009**, *42*, 542–552.

(89) Latva, M.; Takalo, H.; Mukkala, V.; Matachescu, C.; Rodríguez-Ubis, J. C.; Kankare, J. *J. Lumin.* **1997**, *75*, 149–169.